Research Square

Preprints are preliminary reports that have not undergone peer review.
They should not be considered conclusive, used to inform clinical practice,
or referenced by the media as validated information.

Morroniside Ameliorates Hyperuricemic Nephropathy in Mice: Integrated Evidence from Transcriptomic Reanalysis, Molecular Docking, and Experimental Validation

Yao Chen
College of First Clinical Medicine, Shandong University of Traditional Chinese Medicine, Jinan, Shandong, China

guijie Ma
Shiyan Hospital of Integrated Traditional Chinese and Western Medicine

Yinzhong Dai
Department of Nephrology, Xiyuan Hospital, China Academy of Chinese Medical Sciences

Junwei Gao
Department of Nephrology, Ningbo Municipal Hospital of Traditional Chinese Medicine

Yuhua Qiao
Hebei Provincial Key Laboratory of Portal Hypertension and Cirrhosis, Xingtai People's Hospital

Peng Liu
drliupeng@sina.cn

Department of Nephrology, Xiyuan Hospital, China Academy of Chinese Medical Sciences

Article

Keywords: hyperuricemic nephropathy, morroniside, renal inflammation, NF-κB p65, NLRP3

Posted Date: October 22nd, 2026

DOI: https://doi.org/10.21203/rs.3.rs-11063668/v1

License: This work is licensed under a Creative Commons Attribution 4.0 International License.
Read Full License

Additional Declarations: No competing interests reported.

Abstract

Persistent hyperuricemia can promote renal injury through sustained inflammatory signaling. We investigated whether morroniside (MOR) ameliorates hyperuricemic nephropathy (HN) and whether its effects are associated with NF-κB p65/NLRP3 signaling. Molecular docking and reanalysis of the independent kidney transcriptomic dataset GSE190205 were combined with studies in potassium oxonate/adenine-induced HN mice and uric acid-challenged HK-2 cells. Transcriptomic reanalysis showed enrichment of TNF-α/NF-κB, NOD-like receptor, inflammasome-related and pyroptosis-associated programs in untreated HN kidneys. MOR reduced serum uric acid, serum creatinine and urinary albumin-to-creatinine ratio, improved renal histopathology, and decreased inflammatory mediators and levels of phosphorylated NF-κB p65, NLRP3, caspase-1, IL-1β and IL-18. Bay 11-7082 produced broadly concordant effects, and combined treatment further suppressed inflammatory signaling in HK-2 cells.These findings indicate that MOR attenuates renal inflammation and injury in HN in association with suppression of NF-κB p65/NLRP3-related signaling.

1. Introduction

Uric acid (UA) is derived from both dietary purines and endogenous purine synthesis, while circulating UA levels reflect the balance between its production and elimination[1]. When this balance shifts toward accumulation, particularly because renal clearance is impaired, serum uric acid (SUA) rises and hyperuricemia (HUA) develops[2,3]. Over the nearly two decades preceding 2023, HUA prevalence rose by approximately 6 percentage points among adult men and 5 percentage points among adult women[4]. Because the kidneys are central to urate handling and metabolic homeostasis, persistent elevation of UA can gradually compromise renal function and promote the development of hyperuricemic nephropathy (HN), which has also become increasingly common[5,6]. HN may involve abnormal tubular urate handling, reduced glomerular filtration, interstitial fibrosis, and, in some patients, nephrolithiasis[7,8]. Recent advances in HN research have expanded our understanding of its underlying mechanisms, highlighting several contributors to disease progression, including renal inflammation, tubular epithelial–mesenchymal transition, and crystal deposition[9–11]. Among these, chronic inflammation is an important pathogenic feature of HN and is prevalent in a variety of renal diseases[12]. Increasing evidence suggests that HUA may accelerate kidney injury by maintaining a chronic inflammatory state. Elevated circulating UA levels can induce inflammatory signaling and promote the production of diverse cytokines, including interleukins (ILs) such as IL-1β and IL-6, as well as TNF-family cytokines such as TNF-α, thereby aggravating renal inflammatory damage[13–15]. The nuclear factor-κB (NF-κB) pathway can be activated by various stimuli through two major routes, thereby promoting immune cell infiltration and increasing the expression of inflammatory mediators in the kidney[16]. In the canonical pathway, phosphorylation of the IκB kinase (IKK) complex represents a key regulatory event. NF-κB p65 (also known as RelA), a major component of the NF-κB family, is an important mediator of inflammation[17,18]. Normally, NF-κB activity is restrained by IκBα-mediated cytoplasmic retention of the p65/p50 heterodimer, maintaining the

transcription factor in a quiescent state[19]. Activation of IKK shifts NF-κB away from its resting state by first phosphorylating IκBα. This modification marks IκBα for ubiquitination and subsequent proteasomal degradation, allowing the heterodimer to be released[20,21]. This process subsequently enhances the transcription of multiple pro-inflammatory genes[22]. In parallel, the NLRP3 inflammasome functions as another critical inflammatory platform involved in renal injury. This multiprotein complex consists of NLRP3, the adaptor protein ASC, and pro-caspase-1[23]. This brings pro-caspase-1 molecules into close proximity, facilitating their autocatalytic processing and activation. Activated caspase-1 then converts pro-IL-1β and pro-IL-18 into their mature forms[24]. Moreover, previous studies have demonstrated that IL-1βand NLRP3 inflammasome priming are linked to NF-κB signaling, which promotes transcription of NLRP3 and pro-IL-1β and may thereby amplify downstream inflammatory responses[25,26]. Inflammatory and cell-death pathways are also involved in UA-mediated injury. Evidence summarized in previous reviews indicates that soluble UA can stimulate NF-κB and MAPK signaling and increase inflammatory cytokine production[27]. In human renal tubular epithelial cells (HK-2), UA stimulation has been reported to enhance NF-κB p65 activation[28], which is one of the reasons we selected it as the target of observation. Beyond inflammatory signaling, altered tubular urate handling may also contribute to HN. A recent study showed that renal METTL14 overexpression enhanced m6A modification of Glut9 mRNA, accelerated its degradation, reduced GLUT9 expression, and attenuated UA-induced fibrotic injury in renal tubular epithelial cells[29]. Notably, the uricosuric agent benzbromarone has been shown to ameliorate this injury, highlighting the therapeutic potential of the METTL14-GLUT9 axis as a novel target and mechanism. The path forward, however, presents challenges. The balance of urate reabsorption and excretion is governed by a network of transporters—URAT1 and GLUT9 for reabsorption; ABCG2 and OATs for excretion. While lesinurad serves as an effective dual-action urate transporter inhibitor, its benefits do not extend to patients with a glomerular filtration rate < 45 mL/min, which underscores the need for alternative therapeutic strategies[30]. Given the limitations of existing medications—such as the cardiovascular risks associated with febuxostat and hypersensitivity reactions to allopurinol, research into natural compounds has shown significant momentum[31]. Therefore, it is imperative to find an effective treatment for HN.

Morroniside (MOR) is a naturally occurring iridoid glycoside. Previous studies have reported protective effects of MOR in cardiomyocytes [32] and renal cells [33], as well as anti-inflammatory and antioxidant effects [34]. In the MCAO-induced stroke model, MOR mediates neuroprotective effects by promoting M2 microglial polarization and enhancing IL-10 levels[35]. In non-alcoholic steatohepatitis, MOR ameliorates liver injury through AMPKα-mediated lipophagy activation coupled with NLRP3 inflammasome suppression[36]. Furthermore, *in vivo* studies reveal that MOR improves gastrointestinal dysfunction through hypothalamic-pituitary-adrenal axis modulation[37]. In fact, our previous research found that MOR exhibited potential therapeutic effects in the KKAy mouse model and in HK-2 cells[38]. MOR is a major bioactive constituent of *Cornus officinalis Sieb. et Zucc.*, a medicinal herb commonly used in traditional formulations for renal disorders. Nevertheless, how MOR modulates renal inflammation and influences the progression of HN remains incompletely understood. To examine this question, molecular docking

was first used to estimate potential interactions between MOR and selected molecular targets[39]. Experimental studies were then performed to assess the anti-inflammatory effects of MOR in HN and to explore the signaling mechanisms involved. On the basis of the available evidence and our preliminary observations, we hypothesized that MOR may alleviate HN by suppressing NF-κB p65/NLRP3 signaling. The mechanistic diagram is shown in Fig. 1 (created using Figdraw2.0).

2. Materials and Methods

2.1. HN Mouse Model and Drug Administration

At acquisition, male C57BL/6J mice (Beijing Vital River Laboratory Animal Technology Co., Ltd., Beijing, China) were seven weeks old and weighed 20 ± 2 g. Each procedure was individually performed by a different researcher randomly assigned from among YC, GM, and YD. The rationale for model selection is detailed in Section 4. The modeling protocol and validation methods were performed as previously described. Mice were maintained under standard laboratory conditions[40]. A priori power analysis using preliminary data (α = 0.05, power = 80%) yielded a minimum requirement of eight mice per group to detect the expected treatment effect on primary outcomes. To compensate for potential attrition, the final sample size was set to ten per group. Only healthy, male C57BL/6J mice that successfully completed the acclimation period were included. Mice in the HN-related groups were required to show validated model induction, confirmed by elevated serum uric acid and creatinine. Animals were to be excluded if they developed severe intercurrent illness, met pre-set humane endpoints, or experienced critical procedural complications.

After a 1-week acclimation period, 40 mice were randomly allocated to four groups, with 10 animals in each group: control, HN, HN + MOR, and HN + Bay 11-7082. To establish HN, potassium oxonate (2400 mg/kg; P9770, Solaibao, Beijing, China) together with adenine (160 mg/kg; A8330, Solaibao, Beijing, China) was administered orally once daily for 3 consecutive weeks; control mice and HN mice received an equivalent volume of distilled water[41]. Mice in the HN + MOR group were treated with MOR (50 mg/kg/day, Nature Standard Biotechnology, Shanghai, China) by gavage, while mice in the HN + Bay 11-7082 group received Bay 11-7082 (20 mg/kg/day, B5556, Sigma-Aldrich, St. Louis, USA) via tail vein injection. To control for the injection procedure, mice in the other groups received an equivalent volume of the corresponding Bay 11-7082 vehicle by tail vein injection on the same schedule. After 3 weeks of drug treatment, all mice underwent surgery for blood collection via cardiac puncture and kidney tissue excision for subsequent experiments. Before the procedure, mice were anesthetized by intraperitoneal injection of 1% pentobarbital at 40 mg/kg. Animal death was confirmed by the cessation of heartbeat and respiration for more than 3 min after the procedure.

Humane endpoints were defined in advance in accordance with ARRIVE 2.0[42]. Mice showing > 20% body-weight loss, severe lethargy or unresponsiveness, inability to maintain basic self-care, or severe distress unrelated to the intended model were to be euthanized with an overdose of pentobarbital sodium. No animals met these criteria, and all animals completed the study.

All animal experimental procedures were approved by the Ethics Committee of the China-Japan Friendship Institute of Clinical Medical Sciences (approval No. zryhyy21-22-01-09). All experiments were performed in accordance with relevant institutional guidelines and regulations and were reported in accordance with the ARRIVE 2.0 guidelines.

2.2. HK-2 Cell Culture and Morroniside Treatment

HK-2 cells used in this experiment were obtained from Prof. F.Y. Lan of the Chinese University of Hong Kong through a research donation. The rationale for model selection is detailed in Section 4. Cell culture conditions were consistent with those described in our previous study[5]. HK-2 cells were exposed to UA (1.2 mM, U2625, Sigma-Aldrich, St. Louis, USA), followed by treatment with MOR (1 μM, 2 μM, and 4 μM) or Bay 11-7082 (10 μM) for 24 h. Based on existing studies, preliminary concentration ranges for UA and MORwere selected[5,33]. The optimal concentrations for experimentation were subsequently determined using the CCK-8 assay (Mei5 Biotechnology, Beijing, China).

2.3. Molecular Docking

The NF-κB p65 protein entry was identified in UniProt (https://www.uniprot.org/) using 'Transcription factor p65' as the keyword and '*Homo sapiens*' as the species. Human NF-κB p65 (RELA; UniProt accession Q04206; PDB ID: 6NV2; resolution: 1.13 Å) was identified as the target protein. Structural coordinates for the target protein were retrieved from the RCSB Protein Data Bank (PDB; https://www.rcsb.org/) and prepared for molecular docking. The three-dimensional structure of morroniside (MOR; PubChem CID 11228693) was obtained from PubChem (https://pubchem.ncbi.nlm.nih.gov/). Docking was then carried out using CB-Dock2 (https://cadd.labshare.cn/cb-dock2/). The binding affinity was estimated based on the Vina score, with more negative Vina scores indicating stronger predicted binding affinity[43]. Additionally, we conducted molecular docking analyses for Bay 11-7082 (PubChem CID: 5353431) with NF-κB p65, MOR with NLRP3 (Q96P20, 8ZEM), and MOR with each of the following targets: caspase-1 (P29466, 1RWK), IL-1β (P14778, 1ITB), and IL-18 (Q14116, 1J0S).

2.4. Public Transcriptomic Dataset Acquisition and Bioinformatics Analysis

The publicly available mouse kidney RNA-sequencing dataset GSE190205 was obtained from the NCBI Gene Expression Omnibus. Only untreated control (C2, C4, and C5) and untreated HN (M4, M8, and M12) samples were included (n = 3 per group). Following aggregation of duplicated entries by gene symbol, genes with FPKM > 1 in at least three of the six samples were retained, resulting in 13,582 genes from 55,253 unique gene symbols. FPKM values were subsequently transformed as log2(FPKM + 1). Principal component analysis and Pearson correlation analysis were used to assess global transcriptional patterns and sample consistency.

The limma package was applied to identify differentially expressed genes, followed by Benjamini–Hochberg adjustment for multiple comparisons (FDR < 0.05 and |log2 fold change| ≥ 1). Preranked GSEA

was performed using limma-moderated t statistics. Sample-level scores were calculated by ssGSEA for predefined NF-κB (Chuk, Tlr4, Traf6, Tnf, Ikbkb, Nfkbia, Ripk1, Il6, Cxcl1, Ccl2, Nfkb1, Nfkb2, Relb, Rela, and Myd88) and NLRP3 inflammasome/pyroptosis (Nlrc4, Nlrp3, Pycard, Il1b, Gsdmd, Aim2, Casp1, Txnip, P2rx7, and Il18) modules; only genes detectable in the original matrix were included. Spearman correlation analysis assessed associations with Havcr1, Lcn2, Col1a1, Fn1, and Acta2. Heatmaps used row-wise Z-score-standardized expression values. Transcriptomic datasets were processed and analyzed in R (version 4.6.1). P values generated from correlation tests were adjusted for multiple testing according to the Benjamini–Hochberg procedure.

2.5. Biochemical Assays

Blood and urine were collected at predefined time points following treatment. SUA and serum creatinine (Scr) were measured, while the urinary albumin-to-creatinine ratio (UACR) was calculated from the corresponding urinary measurements(Mei5 Biotechnology Co., Beijing, China).

2.6. Histopathology and Immunohistochemistry

Renal specimens were processed into 3-μm paraffin sections after fixation in 10% neutral buffered formalin. Renal morphology was examined using Masson's trichrome, hematoxylin and eosin (H&E), and periodic acid–Schiff (PAS) staining. For immunohistochemistry, sections underwent routine antigen retrieval and blocking before exposure to antibodies against IL-1β (1:20, sc-52012), IL-6 (1:20, sc-130326), and TNF-α (1:50, sc-52746), all from Santa Cruz Biotechnology (CA, USA) at room temperature for 2 h. Immunoreactivity was developed with 3,3'-diaminobenzidine (DAB), followed by hematoxylin counterstaining and microscopic evaluation.

2.7. Immunofluorescence Staining

Renal immunofluorescence was performed using antibodies against p-NF-κB p65 (1:100, sc-136548, Santa Cruz, CA, USA), NLRP3 (1:100, ab260017, Abcam, Cambridge, MA, USA), and caspase-1 (1:100, ab138483, Abcam, Cambridge, MA, USA). After primary-antibody incubation, an Alexa Fluor 594-labeled secondary antibody (1:1000) was applied, and nuclei were stained with DAPI for 5 min in the dark. Sections were mounted in 80% glycerol and examined by inverted fluorescence microscopy.

Cell-bearing coverslips were immersed in 4% paraformaldehyde for 10 min at 4°C and then rinsed with PBS. After incubation with the indicated primary antibodies, Alexa Fluor 594-labeled secondary antibody was applied. Nuclei were labeled with DAPI for 5 min under light-protected conditions. The coverslips were finally mounted in 80% glycerol and viewed under an inverted fluorescence microscope.

2.8. Western Blotting

Protein lysates from kidney tissue and cultured cells were prepared with radioimmunoprecipitation assay buffer (Servicebio, Wuhan, China), and western blotting was conducted according to our previously reported protocol[33]. Antibodies against IL-1β (sc-52012), NF-κB p65 (sc-8008), p-NF-κB p65 (sc-135769), and β-actin (sc-58673) were purchased from Santa Cruz Biotechnology (Santa Cruz, CA, USA).

Antibodies against NLRP3 (ab260017) and caspase-1 (ab138483) were obtained from Abcam (Cambridge, MA, USA). All primary antibodies were diluted at 1:1000. Protein signals were detected using an iBright CL1000 imaging system (Thermo Fisher Scientific, Waltham, MA, USA), and the relative band intensities were quantified with ImageJ software.

2.9. ELISA-Based Measurement of Inflammatory Cytokines

IL-1β and IL-18 levels were quantified using commercial ELISA kits (Mei5 Biotechnology Co., Beijing, China) according to the manufacturer's instructions.

2.10. RNA Extraction and Quantitative PCR (qPCR) Analysis

Total RNA was isolated from cultured cells and kidney tissues and subsequently converted into cDNA using the RevertAid First Strand cDNA Synthesis Kit (Mei5 Biotechnology Co., Beijing, China). qPCR was conducted with the UltraSYBR Green qPCR Kit on a 7500 Fast Real-Time PCR System (Applied Biosystems, Waltham, MA, USA)[44]. β-Actin served as the internal reference for normalization, and primer sequences are listed in Table 1.

Table 1
Primer sequences used for qPCR analysis

Species	Gene	Forward primer (5'–3')	Reverse primer (5'–3')
Mouse	NLRP3	F: ATTACCCGCCCGAGAAAGG	R: TCGCAGCAAAGATCCACACAG
Mouse	caspase-1	F: CTTGGAGACATCCTGTCAGGG	R: AGTCACAAGACCAGGCATATTCT
Mouse	IL-1β	F: CTTCAGGCAGGCAGTATCACTCAT	R: TCTAATGGGAACGTCACACACCAG
Mouse	β-actin	F: ACCCTAAGGCCAACCGTGAAAAG	R: CATGAGGTAGTCTGTCAGGT
Human	NLRP3	F: CGTGAGTCCCATTAAGATGGAGT	R: CCCGACAGTGGATATAGAACAGA
Human	caspase-1	F: AGGACAAACCGAAGGTGA	R: TGGAAGAGCAGAAAGCGA
Human	IL-1β	F: ATGATGGCTTATTACAGTGGCAA	R: GTCGGAGATTCGTAGCTGGA
Human	β-actin	F: AGGCATCCTCACCCTGAAGTA	R: CACACGCAGCTCATTGTAGA

2.11. Data Analysis and Statistical Validation

Statistical analyses were performed using GraphPad Prism 8.0. Data are presented as mean ± SD. For experiments involving more than two groups, one-way ANOVA was used, followed by Dunnett's multiple-comparisons test for prespecified comparisons against the relevant reference group(s) indicated in each figure legend. $P < 0.05$ was considered statistically significant.

3. Results

3.1. Molecular Docking

CB-Dock2 ranked the top five predicted binding poses, and the top-ranked MOR–NF-κB p65 pose yielded a Vina score of − 7.0 kcal/mol (Fig. 2). The 3D complex and amino acid interactions between MOR and NF-κB p65 are shown in Fig. 2. The molecular docking results demonstrated binding energies of -8.2 kcal/mol for NLRP3, -6.4 kcal/mol for caspase-1, -6.4 kcal/mol for IL-1β, and − 9.3 kcal/mol for IL-18. Additionally, we performed complementary docking between Bay 11-7082 and NF-κB p65, which yielded a binding energy of -6.3 kcal/mol. These results suggest that MOR has a potential binding capacity with NF-κB p65. Using the same molecular docking approach, MOR showed favorable predicted interactions with several inflammation-related proteins, as detailed in Fig. 2.

3.2. Independent Transcriptomic Reanalysis Supports NF-κB/NLRP3-Associated Inflammatory Dysregulation in HN

To explore molecular alterations associated with HN, we performed a secondary analysis of kidney transcriptomic profiles from untreated control and HN mice in the GSE190205 dataset. Principal component and correlation analyses demonstrated clear transcriptional separation between the two groups with good within-group consistency (Fig. 3A, B). Differential expression analysis identified 2,118 upregulated and 497 downregulated genes in HN kidneys, with changes involving kidney injury, fibrosis, inflammation, and pyroptosis-related genes (Fig. 3C, D). GSEA further demonstrated enrichment of TNFα/NF-κB signaling, inflammatory response, NOD-like receptor signaling, and pyroptosis-associated pathways in HN kidneys (Fig. 3E-I).

Consistently, NF-κB and NLRP3 inflammasome/pyroptosis module scores were increased in HN kidneys, accompanied by coordinated alterations in pathway-associated genes (Fig. 3J-M). These module scores were positively associated with kidney injury and fibrosis-related markers, although only the association between the NF-κB score and Lcn2 remained significant after multiple-testing correction (Fig. 3N, O). The integrated expression pattern further supported coordinated inflammatory and kidney injury-related transcriptional changes in HN kidneys (Fig. 3P). Collectively, these findings provide independent transcriptomic support for the disease relevance of NF-κB/NLRP3-associated inflammatory dysregulation in HN.

3.3. MOR Improves Renal Biochemical Indices and Histopathological Injury in HN Mice

We measured Scr, UACR, and SUA levels in mice to evaluate kidney function after treatment with the monomer compound MOR, using Bay 11-7082 as a positive control. Figure 4A–C show that HN mice exhibited significantly higher levels of Scr, SUA, and UACR than control mice. Bay 11-7082 treatment effectively alleviated these abnormalities. Similarly, MOR treatment reduced these levels. To further

verify the nephroprotective effects of MOR, we examined the renal pathology. As shown in Fig. 4D, HN mice displayed prominent renal pathological alterations, characterized by tubular injury, increased collagen deposition, and extracellular matrix accumulation. These abnormalities were markedly attenuated following treatment with MOR or Bay 11-7082. These findings support the nephroprotective effects of MOR in HN mice.

3.4. MOR Reduces Renal Inflammation by Regulating Inflammatory Mediators

Representative immunohistochemical staining showed stronger renal immunoreactivity for TNF-α, IL-6, and IL-1β in HN mice than in controls, whereas staining appeared less intense after MOR or Bay 11-7082 treatment (Fig. 5A). Consistent with these qualitative observations, ELISA showed lower renal IL-1β and IL-18 levels following MOR administration (Fig. 5B). The elevated IL-1β mRNA expression caused by HN was markedly reduced following MOR treatment, and a similar trend was observed after Bay 11-7082 administration. In addition, MOR and Bay 11-7082 treatments both decreased the HN-associated increases in NLRP3 and caspase-1 mRNA levels (Fig. 5C).

3.5. MOR Attenuates Renal Inflammation in HN Mice Through Modulation of the NF-κB p65 Signaling Pathway

Representative immunofluorescence images showed stronger renal signals for p-NF-κB p65, NLRP3, and caspase-1 in HN mice than in controls, whereas these signals appeared weaker after MOR or Bay 11-7082 treatment (Fig. 6A). Western blotting showed concordant changes at the protein level, including a lower p-NF-κB p65/NF-κB p65 ratio and reduced NLRP3, caspase-1, and IL-1β levels after the interventions (Fig. 6B).

3.6. MOR Attenuates Uric Acid-Induced Inflammatory Responses in HK-2 Cells

Similar changes were observed at the cellular level after UA stimulation, with increased expression of these three proteins detected by immunofluorescence staining. MOR treatment significantly reduced their expression (Fig. 7A). Preliminary dose-response experiments were performed to establish the uric acid concentration for subsequent cell studies. p-NF-κB p65 reached its highest level at 1.2 mM UA[5]. Based on previous cell viability experiments, MOR was tested at 1 μM, 2 μM, and 4 μM[45]. To determine whether these concentrations affected basal inflammatory status, HK-2 cells were exposed to MOR alone or in combination with UA, and IL-1β protein expression was assessed (Fig. 7B). MOR alone at 1, 2, and 4 μM did not significantly alter IL-1β expression relative to untreated controls. In contrast, UA stimulation markedly increased IL-1β expression, whereas concomitant MOR attenuated this increase, with the lowest IL-1β level observed at 4 μM. A similar pattern was observed by ELISA (Fig. 7C). UA

exposure increased IL-1β and IL-18 levels, while MOR treatment reduced both inflammatory mediators, with the lowest measured levels generally observed at 4 μM.

3.7. MOR Attenuates NF-κB p65/NLRP3-Related Inflammatory Responses in UA-Challenged HK-2 Cells

Western blot analysis showed that UA stimulation increased the p-NF-κB p65/NF-κB p65 ratio in HK-2 cells, whereas MOR treatment reduced this ratio. UA exposure also increased NLRP3 and caspase-1 protein levels, both of which were reduced after MOR treatment (Fig. 8A). At the transcriptional level, MOR treatment reduced UA-induced increases in NLRP3, caspase-1, and IL-1β mRNA expression (Fig. 8B).

3.8. Combined Treatment Suppresses NF-κB p65/NLRP3-Related Inflammatory Responses in UA-Challenged HK-2 Cells

To verify the involvement of NF-κB p65 signaling, UA-stimulated HK-2 cells were treated with MOR, Bay 11-7082, or their combination. ELISA showed that UA exposure markedly increased IL-1β and IL-18 levels (Fig. 9A). Immunofluorescence staining demonstrated that either MOR or Bay 11-7082 reduced the UA-induced increases in NLRP3, caspase-1, and p-NF-κB p65, while the combined treatment produced the greatest reduction (Fig. 9B). Consistent with these findings, western blot analysis demonstrated lower levels of these proteins, accompanied by a reduced p-NF-κB p65/NF-κB p65 ratio following combined treatment (Fig. 9C). Similar changes were observed at the transcriptional level (Fig. 9D). Collectively, these findings indicate that combined treatment further attenuates NF-κB p65/NLRP3-associated inflammatory signaling in UA-challenged HK-2 cells. Collectively, the concordant effects of MOR and Bay 11-7082 are consistent with involvement of NF-κB-associated signaling, but these data do not establish direct pathway dependence.

4. Discussion

Accumulating evidence has demonstrated an independent association between HUA and the risk of CKD [8,46]. HN, a prevalent clinical complication of HUA, is primarily driven by excessive UA-induced renal inflammation[47]. In addition, HUA is associated with elevated glomerular pressure[48], afferent arteriolopathy[49], and accelerated renal fibrosis[50]. Therefore, developing novel therapeutic strategies to effectively halt the progression of HN has become an urgent priority.

The pleiotropic actions of traditional Chinese medicine have attracted increasing attention[51,52]. MOR, one of its major bioactive constituents, has emerged as a compound of particular interest because of its anti-inflammatory activity. Previous studies have linked MOR to suppression of several inflammation-related pathways. In experimental colitis, MOR attenuated inflammatory injury through inhibition of

STAT3/NF-κB signaling[53]. Previous studies have shown that MOR ameliorates diabetic kidney injury by suppressing the AGE–RAGE axis, including receptor for AGEs, p38 MAPK, and NF-κB signaling, thereby mitigating oxidative stress and renal damage[54]. Emerging evidence indicates that MOR suppresses iNOS and COX-2 expression, ameliorating oxidative stress and inflammation in diabetic murine kidneys[55]. The anti-inflammatory actions of MOR are not confined to the kidney[56]. Previous studies have shown that MOR alleviates neuroinflammation and microglial pyroptosis in experimental ischemic injury models. MOR treatment was associated with decreased IL-1β expression and reduced IL-18 levels. In addition, MOR was reported to reduce NLRP3 expression and inhibit caspase-1 activation[57]. Together, these findings suggest that MOR exerts broad anti-inflammatory effects across multiple tissues, with NF-κB-related signaling emerging as a recurrent molecular target. Although MOR has demonstrated anti-inflammatory effects in various disease models, whether it protects against HN-associated renal inflammation remains unclear. Here, we employed an HN mouse model and UA-stimulated HK-2 cells to investigate the renal protective effects of MOR. We found that MOR treatment significantly alleviated inflammatory injury in HN mice.

Inflammatory responses in the kidney play a critical role in HN initiation and progression[58]. Under hyperuricemic conditions, elevated UA levels further intensify renal inflammation by inducing the expression and secretion of multiple pro-inflammatory factors[59,60]. We selected male C57BL/6J mice for this study as this inbred strain is the most widely used model for drug-induced HUA. Its well-defined genetic background and susceptibility to renal pathological phenotypes resembling human disease, particularly crystal nephropathy, make it highly suitable for establishing HN through sequential administration of adenine and potassium oxonate (an inhibitor of uric acid degradation used for hyperuricemia induction)[61,62]. Approximately 95% of glomerular-filtered uric acid is reabsorbed in the proximal tubule. The HK-2 cell line, derived from proximal tubular epithelium, provides a physiologically relevant *in vitro* model for HN studies. Our previous research has consistently demonstrated the reliability of UA-stimulated HK-2 cells in modeling renal pathology, supporting their deliberate selection for this investigation[33,63]. In this study, we initially examined whether MOR could alleviate kidney inflammation and pathological changes in HN mice, improve kidney function, and lower SUA levels. Bay 11-7082, a known NF-κB inhibitor that blocks IKK-β phosphorylation, was employed as a positive control due to its well-documented anti-inflammatory effects[64,65]. Previous research[66] has demonstrated that Bay 11-7082 ameliorates inflammatory responses in diabetic nephropathy rat models by suppressing nearly all proteins examined in our current study, although that investigation did not specifically assess NLRP3 or delineate upstream-downstream relationships. Our work therefore extends these findings by providing mechanistic insights into this pathway. Our results showed that both MOR and Bay 11-7082 significantly reduced SUA and serum creatinine levels in HN mice (Fig. 4). Histopathological assessment revealed prominent inflammatory infiltration, tubular damage, collagen accumulation, and glomerulosclerotic changes in mice exposed to potassium oxonate and adenine. These pathological alterations were markedly attenuated by MOR or Bay 11-7082. Similar renal inflammatory changes have also been documented in the HN model described by Chen et al.[67], supporting a close association

between persistent inflammation and HN progression. Further molecular analyses showed that MOR reduced multiple inflammatory mediators (Fig. 5A–B), indicating a substantial attenuation of the renal inflammatory response. Thus, we hypothesize that MOR may slow HN progression by reducing renal inflammation. Molecular docking has proven to be a valuable tool for predicting the biological activity of compounds by assessing their interactions with potential targets. Our docking results suggest that MOR exhibits strong binding affinity for NF-κB p65[68]. To further investigate how MOR regulates renal inflammation, we focused on the NF-κB p65/NLRP3 axis using both HN mice and UA-challenged HK-2 cells. Previous studies have indicated that elevated uric acid levels activate NF-κB p65 signaling in renal tubular epithelial cells[69]. Meanwhile, NLRP3 serves as a key regulator of renal inflammatory responses[70]. Upon activation, the NLRP3 inflammasome recruits ASC and facilitates caspase-1 maturation, thereby promoting the generation of active IL-1β and IL-18[71,72]. In addition, NF-κB p65-mediated transcriptional regulation enhances the expression of NLRP3 and pro-IL-1β, while also increasing the production of inflammatory cytokines such as TNF-α[73]. Based on this rationale, we further examined whether MOR-mediated inhibition of renal inflammation was associated with modulation of this pathway. In HN mice, adenine/potassium oxonate administration increased renal p-NF-κB p65, NLRP3, and caspase-1 levels. We observed the same phenomenon in UA-stimulated HK-2 cells. Both MOR and Bay 11-7082 reversed these changes, and in cells, we found that a higher concentration of MOR (4 μM) was most effective in mitigating these effects. These observations indicate that the anti-inflammatory activity of MOR may involve regulation of NF-κB p65 phosphorylation and NLRP3 activation. To furtherinvestigate this, we employed a combination of MOR and Bay 11-7082 to treat UA-stimulated HK-2 cells and evaluated whether the combined treatment offered superior efficacy compared to Bay 11-7082 alone. MOR further enhanced the inhibitory response induced by Bay 11-7082, accompanied by a more pronounced decrease in the p-NF-κB p65/NF-κB p65 ratio and reduced levels of NLRP3, caspase-1, and IL-1β. Collectively, these results indicate that MOR may exert anti-inflammatory effects through regulation of NF-κB-associated signaling. We acknowledge certain limitations in our current investigation. Our study primarily focused on the NF-κB/NLRP3 pathway, while other potentially important inflammatory pathways remain unexplored. We acknowledge several limitations. Although the concordant effects of MOR and Bay 11-7082 are consistent with involvement of NF-κB/NLRP3-associated signaling, we did not perform pathway-rescue experiments, genetic manipulation, or direct target-engagement studies; therefore, causal pathway dependence cannot be established. Further investigations are warranted to determine whether MOR regulates inflammatory cytokine production by affecting MAPK signaling (p38, JNK, ERK) or JAK-STAT pathways. These promising directions will be prioritized in our subsequent research. Independent reanalysis of the GSE190205 dataset provided orthogonal support for the disease relevance of the inflammatory network examined in our experimental models. Untreated HN kidneys showed coordinated enrichment of NF-κB-, inflammasome-, and pyroptosis-associated transcriptional programs (Fig. 3). However, given the small sample size and bulk RNA-sequencing design, these findings represent transcriptional associations and do not demonstrate pathway activation or direct regulation by MOR.

5. Conclusions

In conclusion, inflammation is a key driver of HN progression. Our findings indicate that MOR effectively lowers SUA levels and mitigates renal inflammation, while modulation of the NF-κB p65/NLRP3 signaling pathway may contribute to these protective effects.

Declarations

Funding

Funding was provided by the National Natural Science Foundation of China (No. 82274489), the Ningbo Clinical Research Center for Traditional Chinese Medicine Nephrology (No. 2024L001), the Zhejiang Province Traditional Chinese Medicine Key Discipline Construction Project (No. 2024-XK-63), and the Quality Improvement and Innovation Project of Shandong University of Traditional Chinese Medicine (YJSTZCX2026164).

Competing interests

The authors declare no competing interests.

Author Contribution

YC: Conceptualization, Methodology, and Writing – Original Draft. GM: Data Curation, Investigation. YD: Validation. YQ: Funding Acquisition. JG: Resources, Supervision, and Writing – Review & Editing. PL: Project Administration, Funding Acquisition. YC, GM, and YD contributed equally and are recognized as co-first authors. All authors contributed to editorial revisions, read and approved the final manuscript, and agree to be accountable for all aspects of the work.

Data Availability

The transcriptomic dataset analyzed in this study is publicly available in the NCBI Gene Expression Omnibus under accession number GSE190205 (https://www.ncbi.nlm.nih.gov/geo/query/acc.cgi?acc=GSE190205). Other data supporting the findings of this study are available from the corresponding author upon reasonable request.

References

1. Wang, Y. et al. Single photon emission computed tomography/computed tomography imaging of gouty arthritis: A new voice. *J. Transl Int. Med.* **12**, 215–224. https://doi.org/10.2478/jtim-2022-0066 (2024).

2. Keenan, R. T. The biology of urate. *Semin Arthritis Rheum.* **50**, S2–s10. https://doi.org/10.1016/j.semarthrit.2020.04.007 (2020).
3. Liu, P., Ma, G., Wang, Y., Wang, L. & Li, P. Therapeutic effects of traditional Chinese medicine on gouty nephropathy: Based on NF-κB signalingpathways. *Biomed. Pharmacother*. **158**, 114199. https://doi.org/10.1016/j.biopha.2022.114199 (2023).
4. Ngandeu-Singwe, M. et al. Worldwide trends in hyperuricaemia from 2000 to 2023: a systematic review and modelling analysis. *Lancet Rheumatol.* **8**, e346–e362. https://doi.org/10.1016/s2665-9913(25)00344-3 (2026).
5. Liu, P. et al. Zishen Qingre Tongluo Formula Improves Renal Fatty Acid Oxidation and Alleviated Fibrosis via the Regulation of the TGF-β1/Smad3 Signaling Pathway in Hyperuricemic Nephrology Rats. *Biomed Res Int* 2793823 (2021). (2021). https://doi.org/10.1155/2021/2793823
6. Du, Y. et al. Hyperuricemia-Induced Acute Kidney Injury in the Context of Chronic Kidney Disease: A Case Report. *Integr. Med. Nephrol. Androl.* **10**, e00008. https://doi.org/10.1097/imna-d-23-00008 (2023).
7. Strilchuk, L., Fogacci, F. & Cicero, A. F. Safety and tolerability of available urate-lowering drugs: a critical review. *Expert Opin. Drug Saf.* **18**, 261–271. https://doi.org/10.1080/14740338.2019.1594771 (2019).
8. Yang, L., Wang, B., Ma, L. & Fu, P. Traditional Chinese herbs and natural products in hyperuricemia-induced chronic kidney disease. *Front. Pharmacol.* **13**, 971032. https://doi.org/10.3389/fphar.2022.971032 (2022).
9. Yanai, H., Adachi, H., Hakoshima, M. & Katsuyama, H. Molecular Biological and Clinical Understanding of the Pathophysiology and Treatments of Hyperuricemia and Its Association with Metabolic Syndrome, Cardiovascular Diseases and Chronic Kidney Disease. *Int. J. Mol. Sci.* **22** https://doi.org/10.3390/ijms22179221 (2021).
10. Zhang, Y. et al. Hyperuricemia-induced kidney injury: a narrative review of mechanisms and therapeutic advances. *BMC Nephrol.* **26**, 629. https://doi.org/10.1186/s12882-025-04414-7 (2025).
11. Liu, X. et al. Effectiveness of Drug Treatments for Lowering Uric Acid on Renal Function in Patients With Chronic Kidney Disease and Hyperuricemia: A Network Meta-Analysis of Randomized Controlled Trials. *Front. Pharmacol.* **12**, 690557. https://doi.org/10.3389/fphar.2021.690557 (2021).
12. Wen, L., Yang, H., Ma, L. & Fu, P. The roles of NLRP3 inflammasome-mediated signaling pathways in hyperuricemic nephropathy. *Mol. Cell. Biochem.* **476**, 1377–1386. https://doi.org/10.1007/s11010-020-03997-z (2021).
13. Du, L. et al. Hyperuricemia and its related diseases: mechanisms and advances in therapy. *Signal. Transduct. Target. Ther.* **9**, 212. https://doi.org/10.1038/s41392-024-01916-y (2024).
14. Zhang, Y. et al. Simiao San alleviates hyperuricemia and kidney inflammation by inhibiting NLRP3 inflammasome and JAK2/STAT3 signaling in hyperuricemia mice. *J. Ethnopharmacol.* **312**, 116530. https://doi.org/10.1016/j.jep.2023.116530 (2023).

15. Liu, Y. et al. Coptisine protects against hyperuricemic nephropathy through alleviating inflammation, oxidative stress and mitochondrial apoptosis via PI3K/Akt signaling pathway. *Biomed. Pharmacother*. **156**, 113941. https://doi.org/10.1016/j.biopha.2022.113941 (2022).
16. Tan, R. Z. et al. Neuropeptide Y protects kidney from acute kidney injury by inactivating M1 macrophages via the Y1R-NF-κB-Mincle-dependent mechanism. *Int. J. Biol. Sci.* **19**, 521–536. https://doi.org/10.7150/ijbs.80200 (2023).
17. Choi, M. C., Jo, J., Park, J., Kang, H. K. & Park, Y. NF-κB Signaling Pathways in Osteoarthritic Cartilage Destruction. *Cells* **8** https://doi.org/10.3390/cells8070734 (2019).
18. Tan, R. Z. et al. Quercetin protects against cisplatin-induced acute kidney injury by inhibiting Mincle/Syk/NF-κB signaling maintained macrophage inflammation. *Phytother Res.* **34**, 139–152. https://doi.org/10.1002/ptr.6507 (2020).
19. Mankan, A. K., Lawless, M. W., Gray, S. G., Kelleher, D. & McManus, R. NF-kappaB regulation: the nuclear response. *J. Cell. Mol. Med.* **13**, 631–643. https://doi.org/10.1111/j.1582-4934.2009.00632.x (2009).
20. Kim, S. E., Kawaguchi, K., Hayashi, H., Furusho, K. & Maruyama, M. Remission Effects of Dietary Soybean Isoflavones on DSS-Induced Murine Colitis and an LPS-Activated Macrophage Cell Line. *Nutrients* **11** https://doi.org/10.3390/nu11081746 (2019).
21. Ye, X. et al. Alpha-ketoglutarate ameliorates age-related and surgery induced temporomandibular joint osteoarthritis via regulating IKK/NF-κB signaling. *Aging Cell.* **23**, e14269. https://doi.org/10.1111/acel.14269 (2024).
22. Bai, Y. et al. Identification of functional heterogeneity of immune cells and tubular-immune cellular interplay action in diabetic kidney disease. *J. Transl Int. Med.* **12**, 395–405. https://doi.org/10.2478/jtim-2023-0130 (2024).
23. Yuan, Y. et al. Circulating exosome long non-coding RNAs are associated with atrial structural remodeling by increasing systemic inflammation in atrial fibrillation patients. *J. Transl Int. Med.* **12**, 106–118. https://doi.org/10.2478/jtim-2023-0129 (2024).
24. Lv, S., Wang, H. & Li, X. The Role of the Interplay Between Autophagy and NLRP3 Inflammasome in Metabolic Disorders. *Front. Cell. Dev. Biol.* **9**, 634118. https://doi.org/10.3389/fcell.2021.634118 (2021).
25. Wang, D. et al. Eurycoma longifolia alkaloid components ameliorate hyperuricemic nephropathy via regulating serum uric acid level and relieving inflammatory reaction. *J. Nat. Med.* **77**, 867–879. https://doi.org/10.1007/s11418-023-01729-3 (2023).
26. Zhang, C. & Yang, Y. Targeting toll-like receptor 4 (TLR4) and the NLRP3 inflammasome: Novel and emerging therapeutic targets for hyperuricaemia nephropathy. *Biomol. Biomed.* **24**, 688–697. https://doi.org/10.17305/bb.2023.9838 (2023).
27. Wang, T. et al. Overview of pharmacodynamical research of traditional Chinese medicine on hyperuricemic nephropathy: from the perspective of dual-regulatory effect on the intestines and kidneys. *Front. Pharmacol.* **16**, 1517047. https://doi.org/10.3389/fphar.2025.1517047 (2025).

28. Liu, Z. et al. Baicalin and baicalein attenuate hyperuricemic nephropathy via inhibiting PI3K/AKT/NF-κB signalling pathway. *Nephrol. (Carlton)*. **28**, 315–327. https://doi.org/10.1111/nep.14159 (2023).
29. Yang, J. et al. METTL14 downregulates GLUT9 through m6A methylation and attenuates hyperuricemia-induced fibrosis in mouse renal tubular epithelial cells. *Int. Immunopharmacol.* **143**, 113308. https://doi.org/10.1016/j.intimp.2024.113308 (2024).
30. Sanchez-Niño, M. D. et al. Lesinurad: what the nephrologist should know. *Clin. Kidney J.* **10**, 679–687. https://doi.org/10.1093/ckj/sfx036 (2017).
31. Bai, Y. et al. Cardiovascular Safety Evaluation of Febuxostat and Allopurinol: Findings from the FDA Adverse Event Reporting System. *J. Clin. Med.* **12** https://doi.org/10.3390/jcm12186089 (2023).
32. Liu, T. et al. Morroniside enhances angiogenesis and improves cardiac function following acute myocardial infarction in rats. *Eur. J. Pharmacol.* **872**, 172954. https://doi.org/10.1016/j.ejphar.2020.172954 (2020).
33. Chen, Y. et al. Morroniside attenuates podocytes lipid deposition in diabetic nephropathy: A network pharmacology, molecular docking and experimental validation study. *Int. Immunopharmacol.* **138**, 112560. https://doi.org/10.1016/j.intimp.2024.112560 (2024).
34. Park, C., Cha, H. J., Lee, H., Kim, G. Y. & Choi, Y. H. The regulation of the TLR4/NF-κB and Nrf2/HO-1 signaling pathways is involved in the inhibition of lipopolysaccharide-induced inflammation and oxidative reactions by morroniside in RAW 264.7 macrophages. *Arch. Biochem. Biophys.* **706**, 108926. https://doi.org/10.1016/j.abb.2021.108926 (2021).
35. Liu, H., Ou, M. X. & Han, Q. Q. Microglial M2 Polarization Mediated the Neuroprotective Effect of Morroniside in Transient MCAO-Induced Mice. *Front. Pharmacol.* **12**, 784329. https://doi.org/10.3389/fphar.2021.784329 (2021).
36. Zhang, C. et al. Morroniside delays the progression of non-alcoholic steatohepatitis by promoting AMPK-mediated lipophagy. *Phytomedicine* **129**, 155703. https://doi.org/10.1016/j.phymed.2024.155703 (2024).
37. Kimura, Y. & Taniguchi, M. Effects of morroniside isolated from Cornus officinalis fruits on functional gastrointestinal disorders and gastric ulcer in mice. *Fitoterapia* **179**, 106249. https://doi.org/10.1016/j.fitote.2024.106249 (2024).
38. Zhu, W. et al. Regulation of renal lipid deposition in diabetic nephropathy on morroniside via inhibition of NF-KB/TNF-a/SREBP1c signaling pathway. *Chem. Biol. Interact.* **385**, 110711. https://doi.org/10.1016/j.cbi.2023.110711 (2023).
39. Liu, Y. et al. CB-Dock2: improved protein-ligand blind docking by integrating cavity detection, docking and homologous template fitting. *Nucleic Acids Res.* **50**, W159–w164. https://doi.org/10.1093/nar/gkac394 (2022).
40. Wang, J. et al. Establishment and optimization of a novel mouse model of hyperuricemic nephropathy. *Ren. Fail.* **46**, 2427181. https://doi.org/10.1080/0886022x.2024.2427181 (2024).
41. Ren, Q. et al. Natural flavonol fisetin attenuated hyperuricemic nephropathy via inhibiting IL-6/JAK2/STAT3 and TGF-β/SMAD3 signaling. *Phytomedicine* **87**, 153552.

https://doi.org/10.1016/j.phymed.2021.153552 (2021).

42. Percie du Sert. The ARRIVE guidelines 2.0: Updated guidelines for reporting animal research. *Br. J. Pharmacol.* **177**, 3617–3624. https://doi.org/10.1111/bph.15193 (2020).
43. Luo, X. et al. Exploring the mechanism of ShenGui capsule in treating heart failure based on network pharmacology and molecular docking: A review. *Med. (Baltim).* **103**, e37512. https://doi.org/10.1097/md.0000000000037512 (2024).
44. Wang, X. et al. Treatment with a PPAR-γ Agonist Protects Against Hyperuricemic Nephropathy in a Rat Model. *Drug Des. Devel Ther.* **14**, 2221–2233. https://doi.org/10.2147/dddt.S247091 (2020).
45. Gao, J. et al. Morroniside Promotes PGC-1α-Mediated Cholesterol Efflux in Sodium Palmitate or High Glucose-Induced Mouse Renal Tubular Epithelial Cells. *Biomed Res Int* 9942152 (2021). (2021). https://doi.org/10.1155/2021/9942152
46. Wu, C. L. et al. Vegan Diet Is Associated with a Lower Risk of Chronic Kidney Disease in Patients with Hyperuricemia. *Nutrients* **15** https://doi.org/10.3390/nu15061444 (2023).
47. Cui, D. et al. Phloretin ameliorates hyperuricemia-induced chronic renal dysfunction through inhibiting NLRP3 inflammasome and uric acid reabsorption. *Phytomedicine* **66**, 153111. https://doi.org/10.1016/j.phymed.2019.153111 (2020).
48. Fan, S. et al. Hyperuricemia and its related histopathological features on renal biopsy. *BMC Nephrol.* **20**, 95. https://doi.org/10.1186/s12882-019-1275-4 (2019).
49. Park, J. H., Jo, Y. I. & Lee, J. H. Renal effects of uric acid: hyperuricemia and hypouricemia. *Korean J. Intern. Med.* **35**, 1291–1304. https://doi.org/10.3904/kjim.2020.410 (2020).
50. Li, Y. et al. Apigenin ameliorates hyperuricemic nephropathy by inhibiting URAT1 and GLUT9 and relieving renal fibrosis via the Wnt/β-catenin pathway. *Phytomedicine* **87**, 153585. https://doi.org/10.1016/j.phymed.2021.153585 (2021).
51. Ma, L., Feng, Z. & Li, P. New Insights into the Use of Traditional Chinese Medicine for Treating Diabetic Kidney Disease by Regulating DNA Methylation. *Integr. Med. Nephrol. Androl.* **11**, e24–00018. https://doi.org/10.1097/imna-d-24-00018 (2024).
52. Chung, J. Y. F., Lan, H. Y. & Tang, P. M. K. New Insights into Traditional Chinese Medicine in Treatment of Diabetic Nephropathy. *Integr. Med. Nephrol. Androl.* **10**, e00026. https://doi.org/10.1097/imna-d-22-00026 (2023).
53. Yuan, J. et al. Protective effects of iridoid glycosides on acute colitis via inhibition of the inflammatory response mediated by the STAT3/NF-κB pathway. *Int. Immunopharmacol.* **81**, 106240. https://doi.org/10.1016/j.intimp.2020.106240 (2020).
54. Lv, G., Lv, X., Tao, Y. & Xu, H. Effect of morroniside on glomerular mesangial cells through AGE-RAGE pathway. *Hum. Cell*. **29**, 148–154. https://doi.org/10.1007/s13577-015-0128-0 (2016).
55. Park, C. H., Noh, J. S., Tanaka, T. & Yokozawa, T. Effects of morroniside isolated from Corni Fructus on renal lipids and inflammation in type 2 diabetic mice. *J. Pharm. Pharmacol.* **62**, 374–380. https://doi.org/10.1211/jpp.62.03.0013 (2010).

56. Xiao, J. et al. Morroniside Inhibits Inflammatory Bone Loss through the TRAF6-Mediated NF-κB/MAPK Signalling Pathway. *Pharmaceuticals (Basel)*. 16. https://doi.org/10.3390/ph16101438 (2023).
57. Ma, Y. et al. Morroniside alleviates neuroinflammation in ischemic injury by mediating microglial pyroptosis via the IL-17/NF-κB/NLRP3 pathway. *Eur. J. Pharmacol.* **1016**, 178622. https://doi.org/10.1016/j.ejphar.2026.178622 (2026).
58. Wang, Y. et al. Clerodendranthus spicatus [Orthosiphon aristatus (Blume) Miq.] maintains uric acid homeostasis via regulating gut microbiota and restrains renal inflammation in hyperuricemic nephropathy. *Front. Pharmacol.* **15**, 1485861. https://doi.org/10.3389/fphar.2024.1485861 (2024).
59. Crawley, W. T., Jungels, C. G., Stenmark, K. R. & Fini, M. A. U-shaped association of uric acid to overall-cause mortality and its impact on clinical management of hyperuricemia. *Redox Biol.* **51**, 102271. https://doi.org/10.1016/j.redox.2022.102271 (2022).
60. Wang, M., Lin, X., Yang, X. & Yang, Y. Research progress on related mechanisms of uric acid activating NLRP3 inflammasome in chronic kidney disease. *Ren. Fail.* **44**, 615–624. https://doi.org/10.1080/0886022x.2022.2036620 (2022).
61. Guan, J. et al. A novel mouse model of hyperuricemia and gouty nephropathy. *Chin. Med. J. (Engl)*. **133**, 2012–2014. https://doi.org/10.1097/cm9.0000000000000964 (2020).
62. Lu, J. et al. Mouse models for human hyperuricaemia: a critical review. *Nat. Rev. Rheumatol.* **15**, 413–426. https://doi.org/10.1038/s41584-019-0222-x (2019).
63. Hu, H. et al. The SGLT2 inhibitor dapagliflozin ameliorates renal fibrosis in hyperuricemic nephropathy. *Cell. Rep. Med.* **5**, 101690. https://doi.org/10.1016/j.xcrm.2024.101690 (2024).
64. Huang, W. C. et al. Decreased Human Platelet Activation and Mouse Pulmonary Thrombosis by Rutaecarpine and Comparison of the Relative Effectiveness with BAY11-7082: Crucial Signals of p38-NF-κB. *Molecules* **27** https://doi.org/10.3390/molecules27020476 (2022).
65. Kandasamy, M. NF-κB signalling as a pharmacological target in COVID-19: potential roles for IKKβ inhibitors. *Naunyn Schmiedebergs Arch. Pharmacol.* **394**, 561–567. https://doi.org/10.1007/s00210-020-02035-5 (2021).
66. Kolati, S. R. et al. BAY 11-7082 ameliorates diabetic nephropathy by attenuating hyperglycemia-mediated oxidative stress and renal inflammation via NF-κB pathway. *Environ. Toxicol. Pharmacol.* **39**, 690–699. https://doi.org/10.1016/j.etap.2015.01.019 (2015).
67. Chen, L. & Lan, Z. Polydatin attenuates potassium oxonate-induced hyperuricemia and kidney inflammation by inhibiting NF-κB/NLRP3 inflammasome activation via the AMPK/SIRT1 pathway. *Food Funct.* **8**, 1785–1792. https://doi.org/10.1039/c6fo01561a (2017).
68. Wang, F. et al. Triptolide is a Promising Therapeutic Approach in Treating Thyroid Cancer Based on in silico and in vitro Experiment. *Drug Des. Devel Ther.* **15**, 4275–4287. https://doi.org/10.2147/dddt.S322502 (2021).
69. Shi, M. et al. Pharmacological inhibition of fatty acid-binding protein 4 alleviated kidney inflammation and fibrosis in hyperuricemic nephropathy. *Eur. J. Pharmacol.* **887**, 173570.

https://doi.org/10.1016/j.ejphar.2020.173570 (2020).

70. Peng, X., Liu, K., Hu, X., Gong, D. & Zhang, G. Hesperitin-Copper(II) Complex Regulates the NLRP3 Pathway and Attenuates Hyperuricemia and Renal Inflammation. *Foods* **13** https://doi.org/10.3390/foods13040591 (2024).
71. Huang, Y., Xu, W. & Zhou, R. NLRP3 inflammasome activation and cell death. *Cell. Mol. Immunol.* **18**, 2114–2127. https://doi.org/10.1038/s41423-021-00740-6 (2021).
72. Fu, J. & Wu, H. Structural Mechanisms of NLRP3 Inflammasome Assembly and Activation. *Annu. Rev. Immunol.* **41**, 301–316. https://doi.org/10.1146/annurev-immunol-081022-021207 (2023).
73. Zhao, Y. et al. Salvianolic acid B inhibits atherosclerosis and TNF-α-induced inflammation by regulating NF-κB/NLRP3 signaling pathway. *Phytomedicine* **119**, 155002. https://doi.org/10.1016/j.phymed.2023.155002 (2023).

Figures

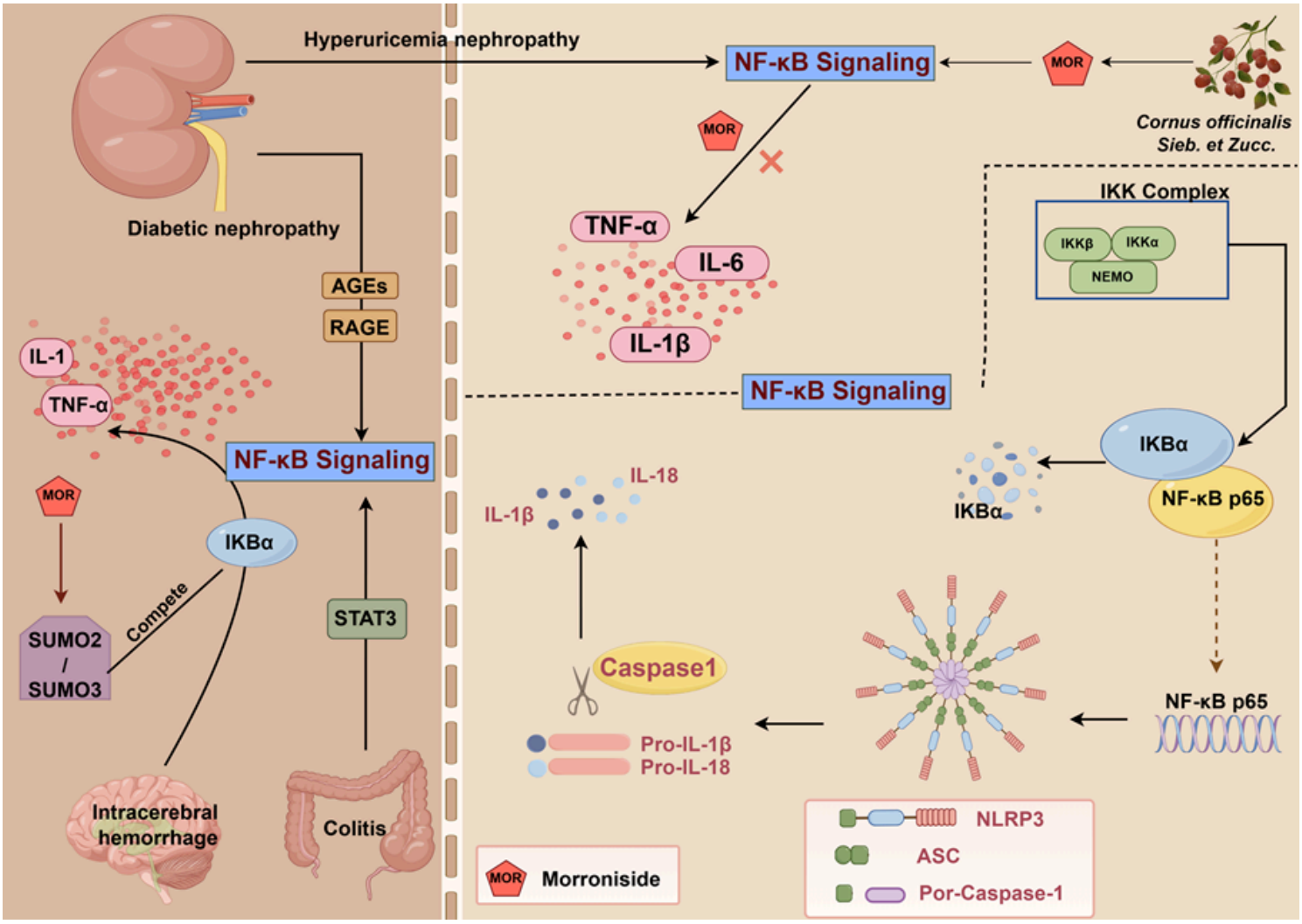


Figure 1

The diagram summarizes selected mechanisms involving NF-κB signaling in different organs and illustrates the proposed pathway through which MOR attenuates renal inflammation in the present study.

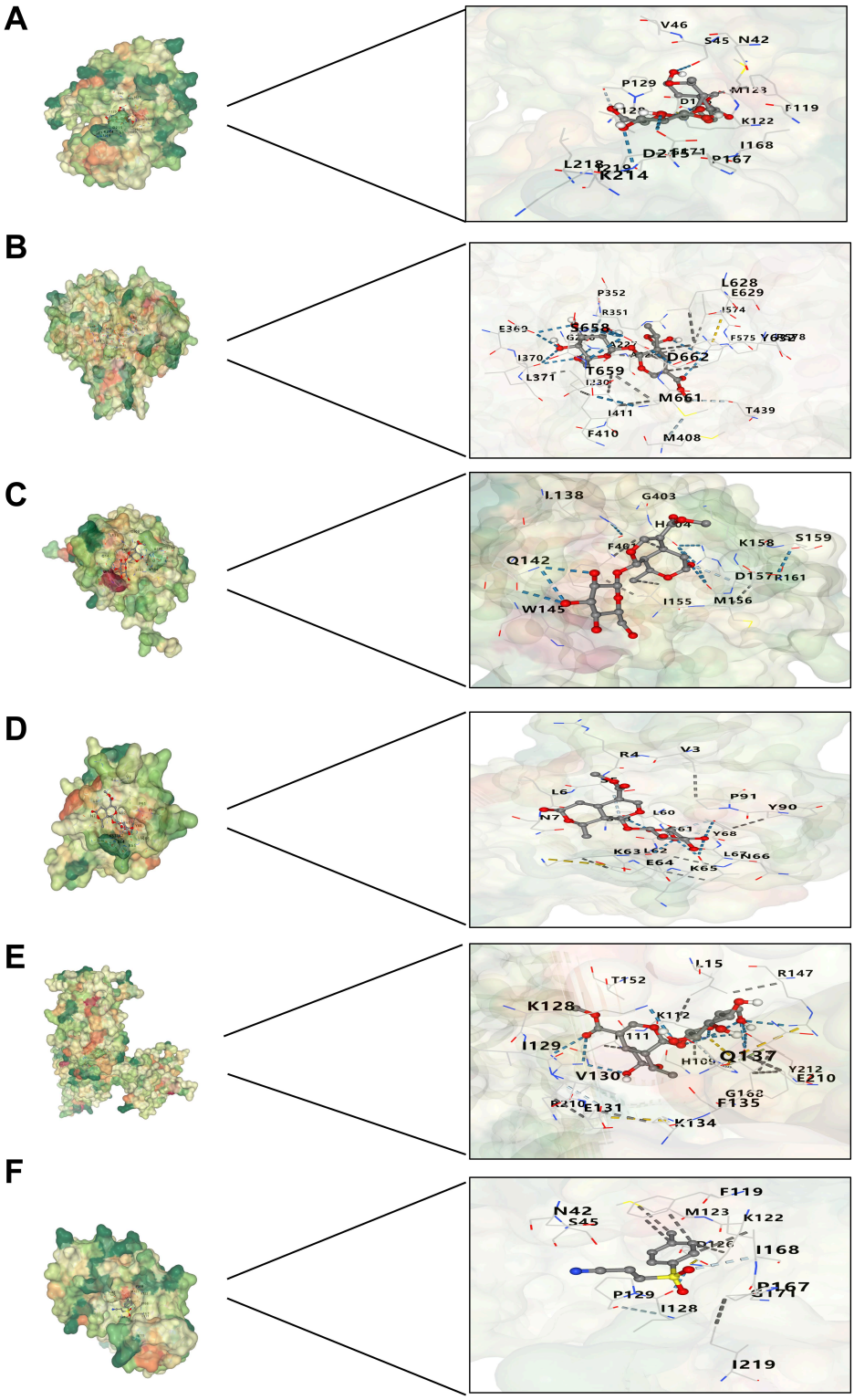


Figure 2

Molecular docking of MOR with inflammation-related targets. Predicted binding modes of MOR with (A) NF-κB p65, (B) NLRP3, (C) caspase-1, (D) IL-1β, and (E) IL-18. (F) Predicted interaction between Bay 11-

7082 and NF-κB p65.

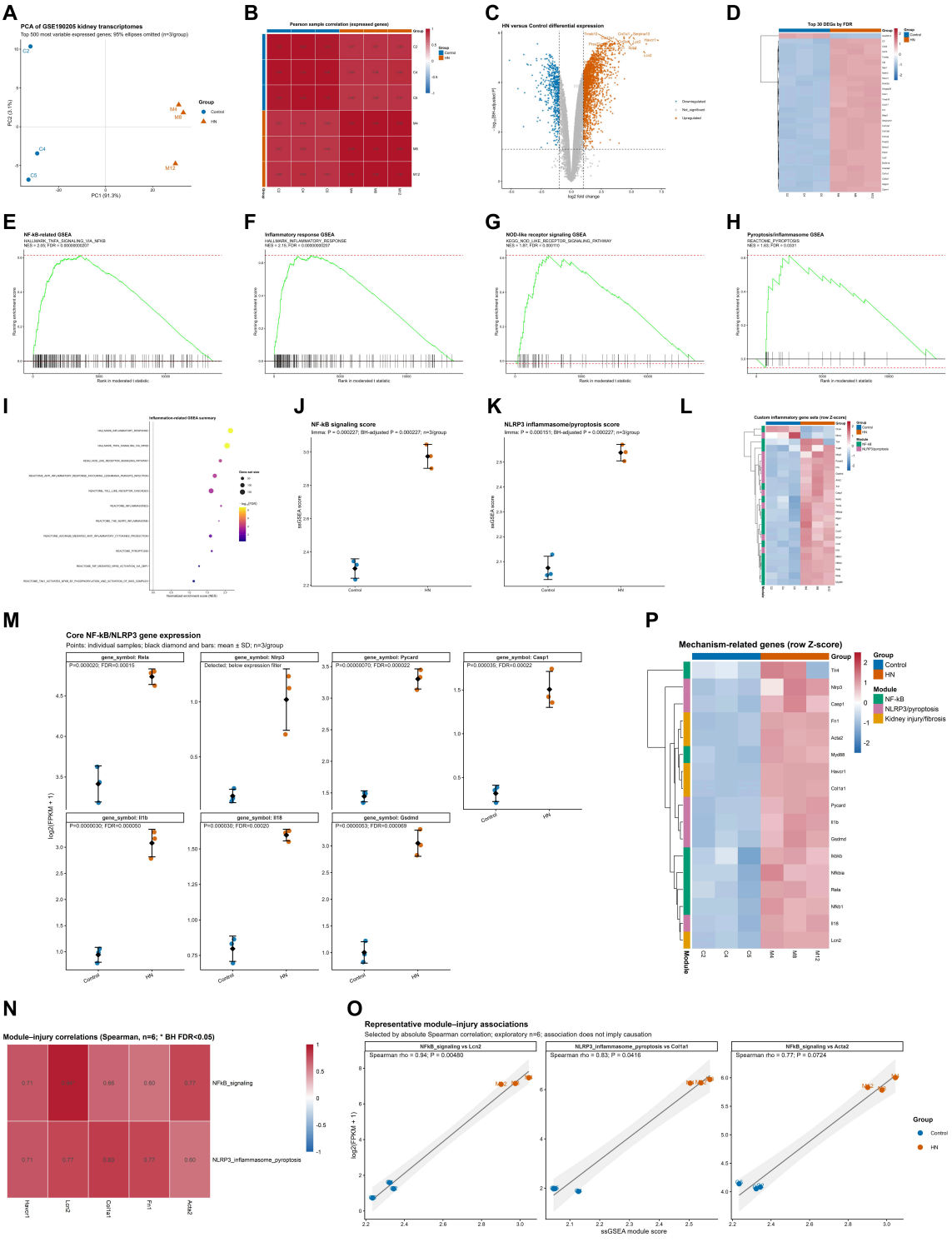


Figure 3

Transcriptomic reanalysis supports NF-κB/NLRP3-associated inflammatory dysregulation in HN kidneys. (A, B) Principal component analysis and Pearson correlation analysis of renal transcriptomes from control and HN mice. (C, D) Differential expression profiles visualized by volcano plot and heatmap

based on the comparison of HN and control samples (FDR < 0.05 and |log2 fold change| ≥ 1). (E–I) Preranked GSEA illustrating representative inflammation- and cell death-related pathways enriched in HN kidneys. (J–L) ssGSEA scores and expression heatmaps for NF-κB- and NLRP3 inflammasome/pyroptosis-related gene modules. (M) Expression profiles of representative genes associated with NF-κB/NLRP3 signaling. Nlrp3 is displayed descriptively because it did not satisfy the predefined low-expression filtering criterion. (N, O) Relationships between inflammatory module scores and genes associated with renal injury or fibrosis. (P) Integrated heatmap of genes related to NF-κB signaling, inflammasome/pyroptosis, and renal injury/fibrosis. Control, untreated control mice; HN, untreated mice with hyperuricemic nephropathy; n = 3 per group.

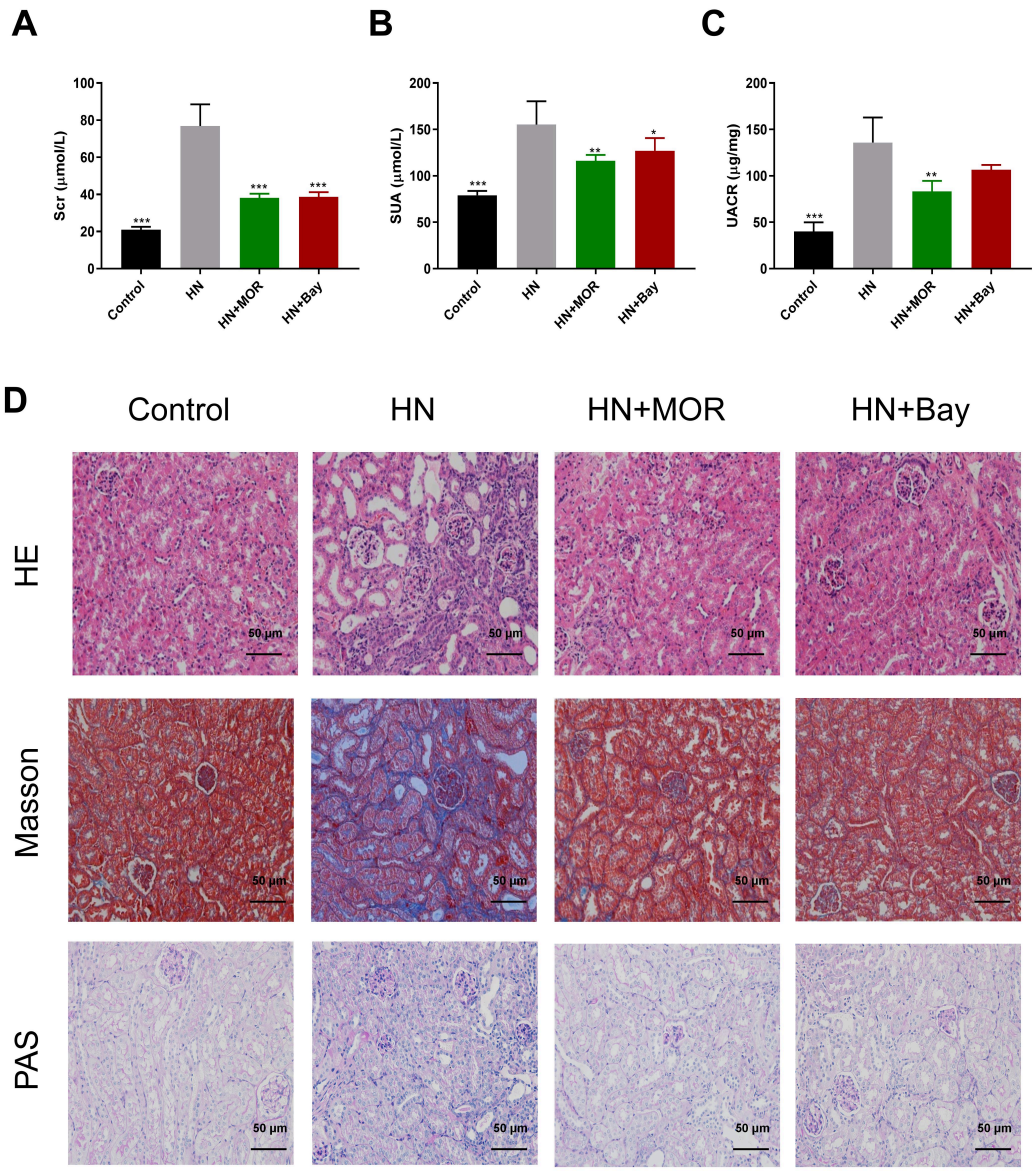


Figure 4

MOR improves renal biochemical indices and histopathological injury in HN mice. (A–C) Scr, SUA, and UACR, respectively, in the indicated groups following 3 weeks of MOR or Bay 11-7082 treatment. Values are shown as mean ± SD (n = 10). Statistical analysis was performed using one-way ANOVA followed by Dunnett's test. Statistical comparisons were made with the HN group, with significance defined as *P <

0.05, **P < 0.01, and ***P < 0.001. (D) Representative renal images stained with H&E, Masson's trichrome, and PAS from each group (magnification, ×200; scale bar = 50 μm).

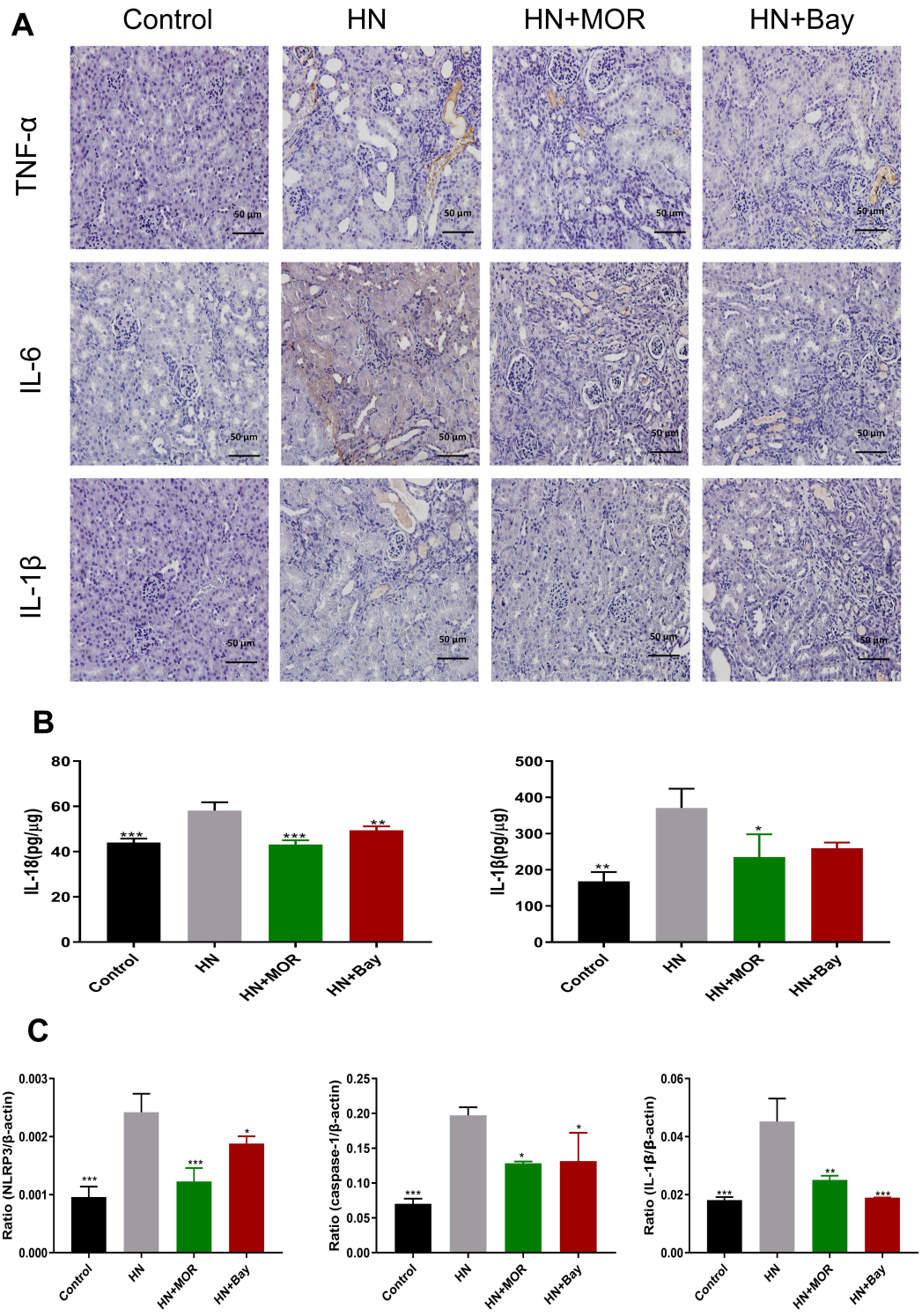


Figure 5

MOR attenuates inflammatory changes in HN mice. (A) Immunohistochemical staining images showing renal expression of TNF-α, IL-6, and IL-1β after 3 weeks of MOR or Bay 11-7082 administration

(magnification, ×200; scale bar = 50 μm). (B) Quantification of renal IL-1β and IL-18 levels by ELISA. (C) Analysis of NLRP3 mRNA expression levels, as well as caspase-1 and IL-1β mRNA expression levels, in the Control, HN, HN + MOR, and HN + Bay groups. Values are shown as mean ± SD (n = 10). Statistical analysis was performed using one-way ANOVA followed by Dunnett's test. Statistical comparisons were made with the HN group, with significance defined as *P < 0.05, **P < 0.01, and ***P < 0.001.

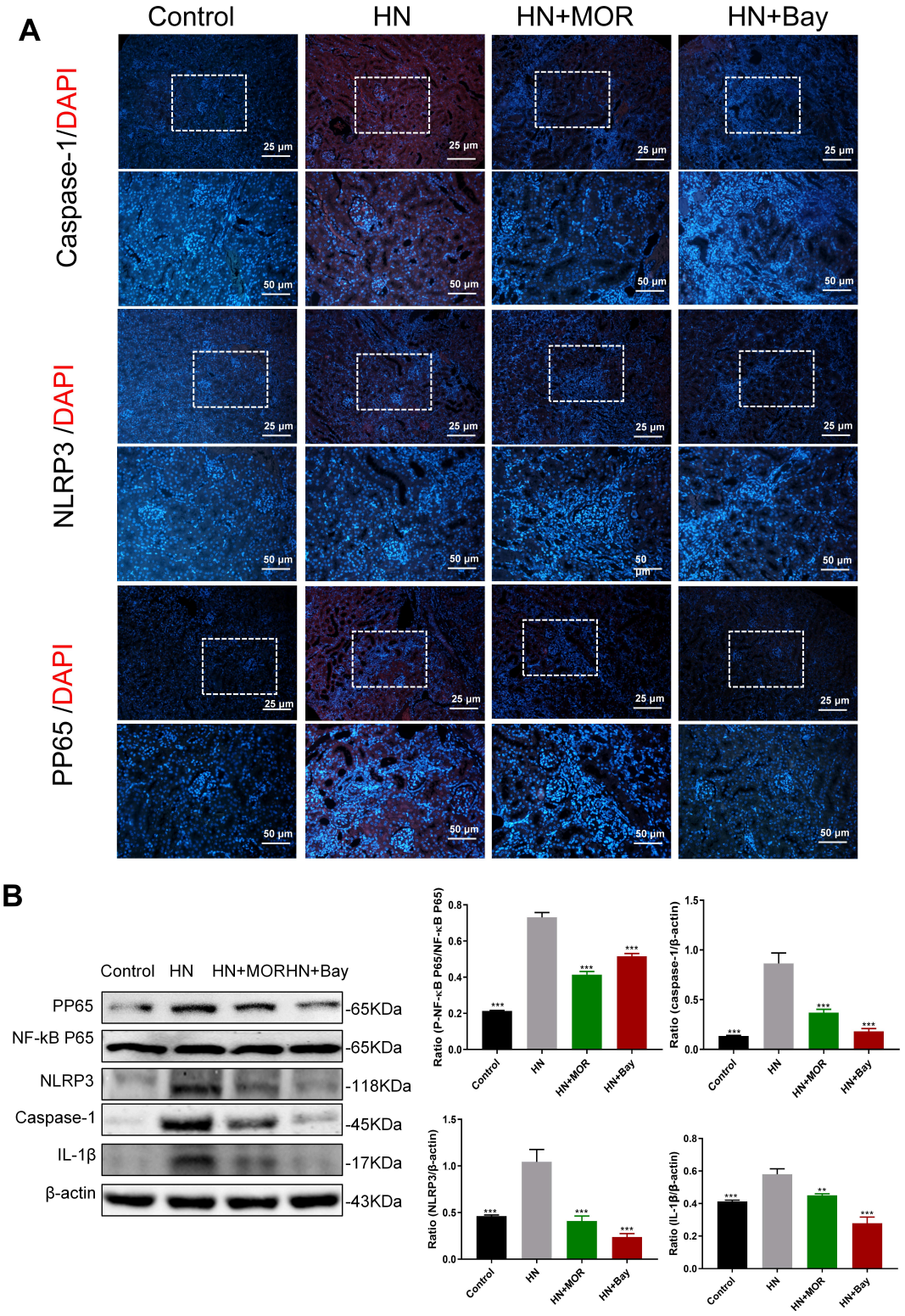


Figure 6

Effect of MOR treatment on NF-κB p65/NLRP3-related inflammatory alterations in HN kidneys. (A) Immunofluorescence staining revealed the distribution of caspase-1, NLRP3, and p-NF-κB p65 in renal sections after 3 weeks of MOR or Bay 11-7082 administration (magnification, ×400/×200; scale bars, 25/50 μm). (B) To assess NF-κB pathway activation, the ratio of phosphorylated to total NF-κB p65 was measured in the Control, HN, HN + MOR, and HN + Bay groups by western blotting. Additionally, the protein levels of NLRP3, as well as those of caspase-1 and IL-1β, were detected using the same assay. Values are shown as mean ± SD (n = 10). Statistical analysis was performed using one-way ANOVA followed by Dunnett's test. Statistical comparisons were made with the HN group, with significance defined as *P < 0.05, **P < 0.01, and ***P < 0.001.

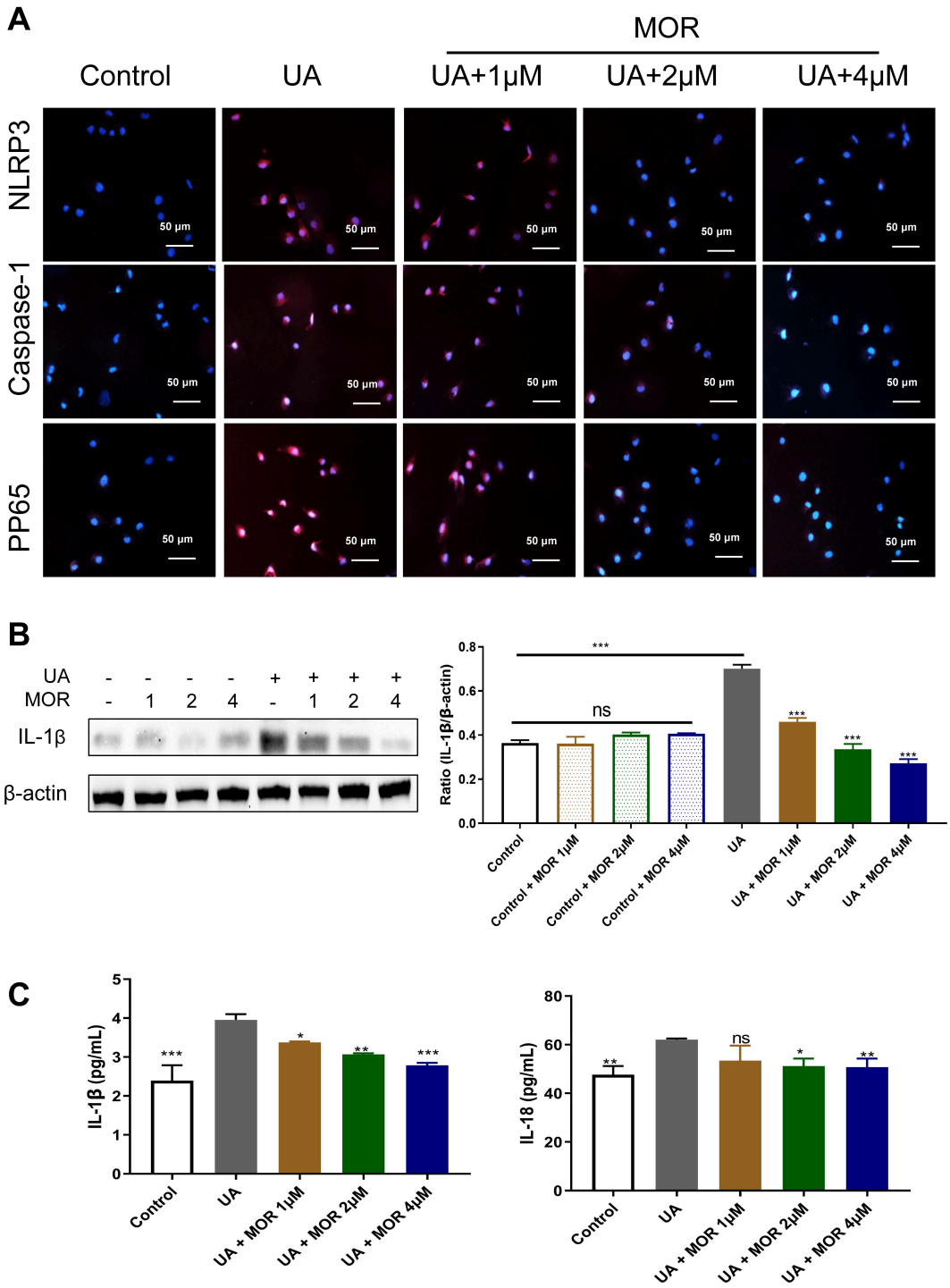


Figure 7

MOR reduces UA-induced inflammatory cytokine expression in HK-2 cells (n = 3). (A) Representative immunofluorescence images of NLRP3, caspase-1, and p-NF-κB p65 in control, UA, UA + MOR (1, 2, 4 μM) groups. (magnification, ×200; scale bar = 50 μm). (B) IL-1β protein expression in the indicated experimental groups. NS represents no significant difference compared with the control group; ***P < 0.001 vs. the UA group. (C) ELISA analysis of IL-1β and IL-18 levels in the indicated experimental groups.

Values are shown as mean ± SD. Statistical analysis was performed using one-way ANOVA followed by Dunnett's test. Statistical comparisons were made with the UA group, with significance defined as *P < 0.05, **P < 0.01, and ***P < 0.001.

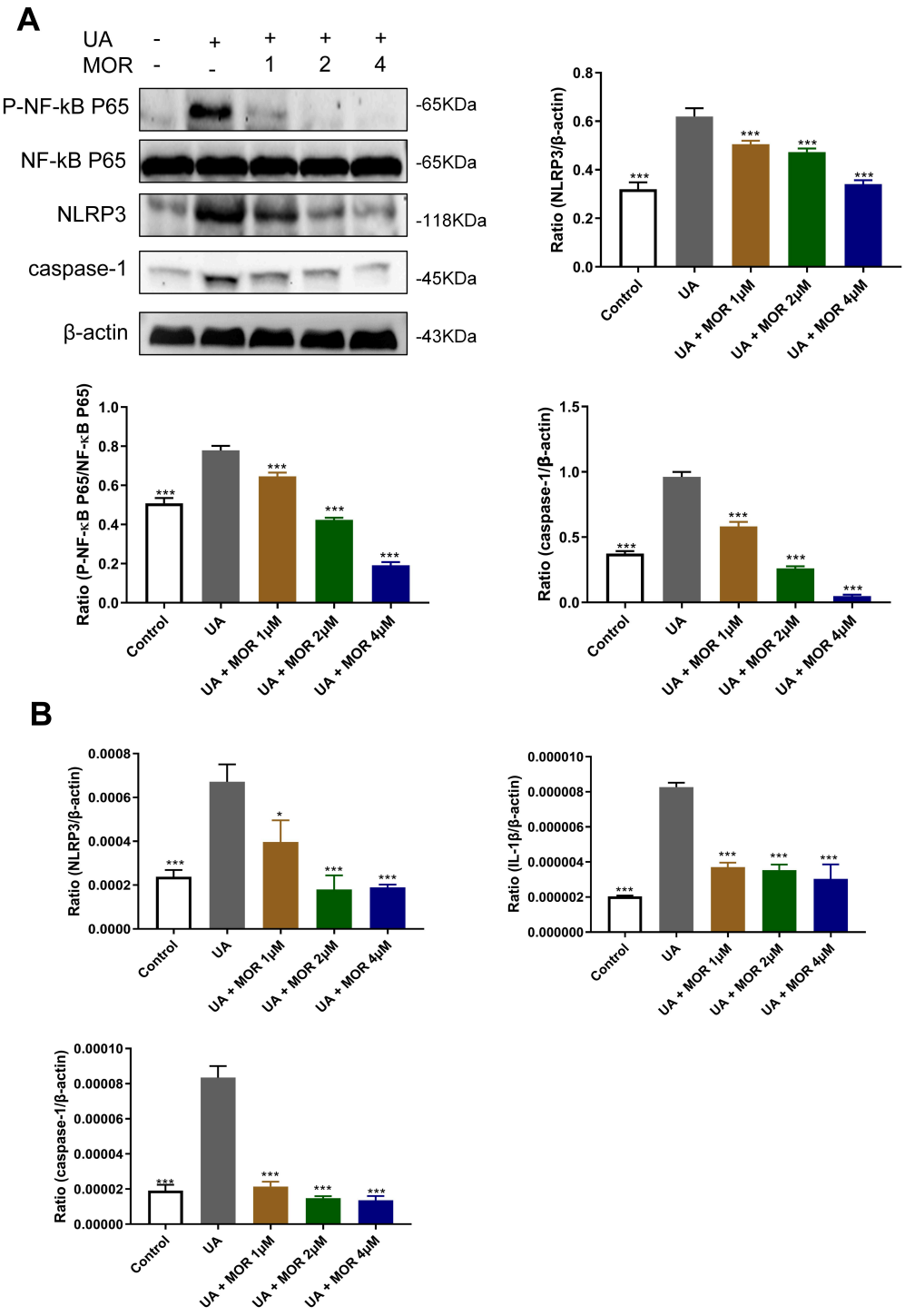


Figure 8

MOR suppresses UA-induced NF-κB p65/NLRP3 inflammatory signaling in HK-2 cells. (A) The ratio of phosphorylated to total NF-κB p65 was measured in the Control, UA, UA + MOR, and UA + Bay groups by western blotting(n = 3). Additionally, the protein levels of NLRP3, as well as those of caspase-1 and IL-1β, were detected using the same assay. (B) Relative mRNA expression of NLRP3, caspase-1, and IL-1β. Values are shown as mean ± SD. Statistical analysis was performed using one-way ANOVA followed by Dunnett's test. Statistical comparisons were made with the UA group, with significance defined as *P < 0.05, **P < 0.01, and ***P < 0.001.

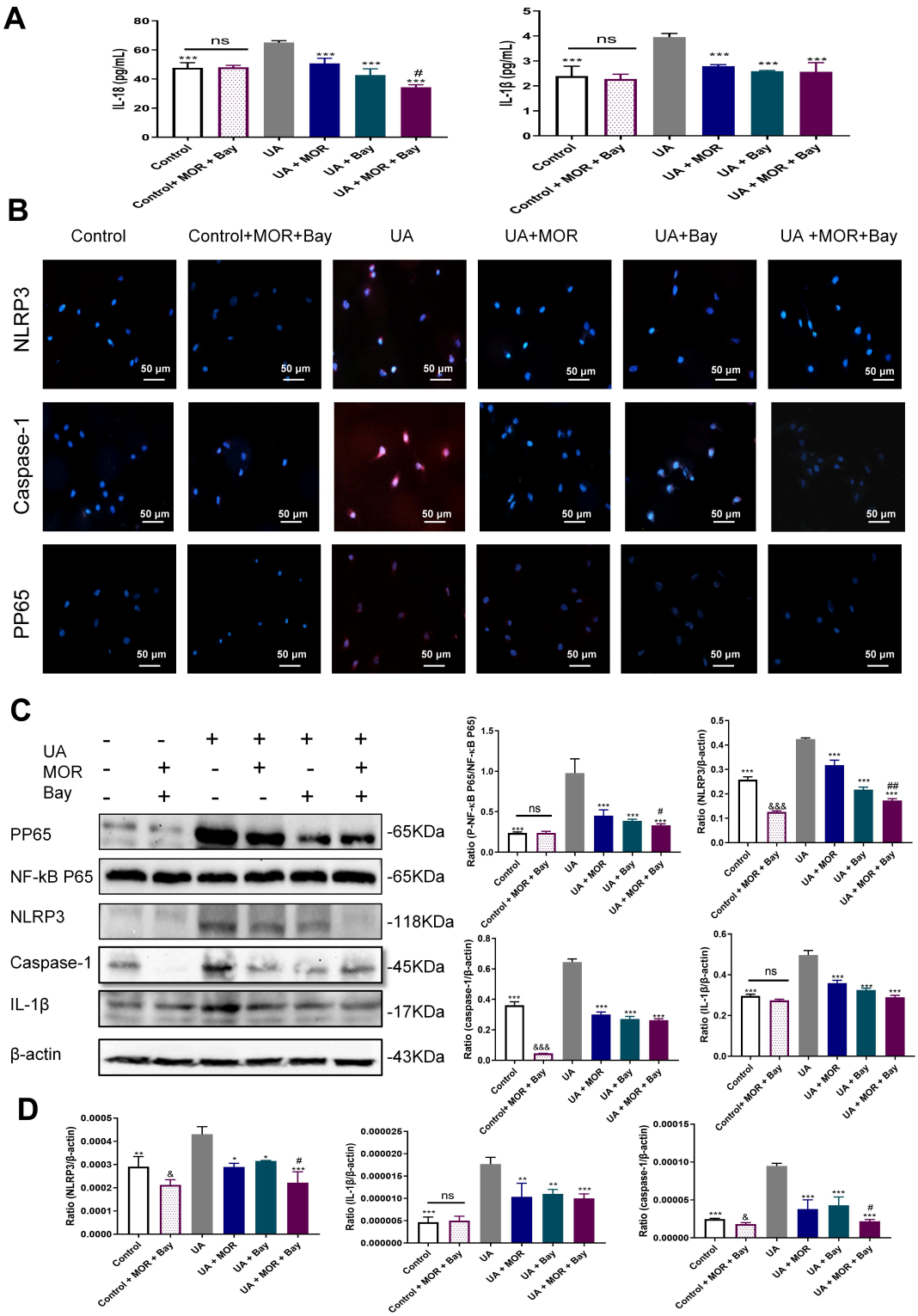


Figure 9

Effects of MOR, Bay 11-7082, and their combination on the UA-induced inflammatory response in HK-2 cells.(A) ELISA analysis of IL-1β and IL-18 levels in the indicated experimental groups. (B) Representative immunofluorescence images of NLRP3, caspase-1, and p-NF-κB p65 in the Control, Control + MOR + Bay, UA, UA + MOR, UA + Bay, and UA + MOR + Bay groups. Magnification, ×200; scale bar = 50 μm. (C) The ratio of phosphorylated to total NF-κB p65 was measured in the Control, UA, UA + MOR, UA + Bay, and UA+MOR+Bay groups (n = 3) by western blotting. Additionally, the protein levels of NLRP3, as well as those of caspase-1 and IL-1β, were detected using the same assay. (D) Relative mRNA expression of NLRP3, caspase-1, and IL-1β. Values are shown as mean ± SD. Control + MOR + Bay group vs. control group, NS. &P < 0.05, &&P < 0.01 and &&&P < 0.001 vs. the control group. *P < 0.05, **P < 0.01 and ***P < 0.001 vs. the UA group. UA + MOR + Bay vs. Control + MOR + Bay, #P < 0.05, ##P < 0.01 and ###P < 0.001. Statistical analysis was performed using one-way ANOVA followed by Dunnett's test.